

Efficient Deep-Blue Organic Light-emitting Diodes with Double-Emission Layers

Ji Hoon Seo^{***a}, Jung Sun Park^a, Bo Min Seo^a, Kum Hee Lee^b, Jung keun Park^b,
Seung Soo Yoon^b, and Young Kwan Kim^{*a}

Abstract

Efficient deep-blue organic light-emitting diodes were demonstrated using 4,4'-bis(9-ethyl-3-carbazovinyleno)-1,1'-biphenyl doped in double-emission layers (D-EMLs). The D-EML system, which consists of 2-methyl-9,10-di(2-naphthyl)anthracene and 1,4-(dinaphthalen-2-yl)-naphthalene as blue hosts, was employed to broaden the recombination zone and to ensure the good confinement of the holes and electrons. The optimized device showed a peak current efficiency of 4.47 cd/A, a peak external quantum efficiency of 4.09%, and Commission Internationale de L'Eclairage coordinates of (0.16, 0.10).

Keywords: Deep-blue organic light-emitting diodes, double-emission layer

1. Introduction

Organic light-emitting diodes (OLEDs) have attracted considerable attention due to their many advantages for use in full-color displays, such as their high brightness, low power consumption, fast response time, wide-view angle, and thinness [1-5]. Many researchers have also reported phosphorescent or fluorescent green and red emitters of high device performance in OLEDs [6-10]. The phosphorescent or fluorescent blue emitters, however, have remained weak in terms of realizing full-color display. In spite of their potential capabilities and 100% internal quantum efficiency, no phosphorescent blue emitters have yet been considered proper candidates for display application due to their short life and insufficient color purity. The deep-blue color is defined as having Commission Internationale d'Eclairage (CIEy) coordinates of <0.15. It is easy to transfer energy to the green and red emitters and to reduce

the power consumption of the full-color OLEDs [11]. Therefore, the deep-blue emitter of high device performance is one of the largest issues in relation to the OLEDs.

OLEDs with double-emission layers (D-EMLs) have exhibited good device efficiency improvement of late [12, 13]. In general, exciton formation zones are generated at the interface of the hole-transporting layer (HTL)/emitting layer (EML) or EML/electron-transporting layer (ETL) in a single EML (S-EML). Therefore, they exhibit narrow emission zones and a negative effect on the efficiency. Eom et al. have successfully improved the efficiency of phosphorescent white OLEDs with D-EML [12]. They reported that efficient charge and exciton confinement is realized by employing charge transport layers. In this paper, efficient deep-blue OLEDs using 2-methyl-9, 10-di(2-naphthyl) anthracene (MADN) and 1,4-(dinaphthalen-2-yl)-naphthalene (DNN) as hosts and 4,4'-bis(9-ethyl-3-carbazovinyleno)-1,1'-biphenyl (BCzVBi) as a dopant are reported. The optimized device with D-EML exhibited higher efficiency and more deep-blue emission compared to the control device.

2. Experiment

Indium-tin-oxide-(ITO)-coated glass was cleaned in ultrasonic baths consisting of acetone, methanol, distilled water, and isopropyl alcohol, respectively, in that order. Thereafter, the precleaned ITO was treated with O₂ plasma

Manuscript Received August 31, 2009; Revised September 16, 2009; Accepted for publication September 25, 2009.

This work was accomplished with support from the ERC program of the Korea Science and Engineering Foundation (KOSEF) grant funded by Korea Ministry of Education, Science, and Technology (MEST) (No. R11-2007-045-03001-0).

* Member, KIDS; ** Student Member, KIDS

Corresponding author: Young Kwan Kim

^a Department of Information Display, Hongik University 72-1 Sangsu-dong, Mapo-ku, Seoul 121-791, Korea

^b Department of Chemistry, Sungkyunkwan University 300 Cheoncheon-dong, Jangan-Gu, Suwon, Gyeonggi-Do 440-746, Korea.

E-mail : kimyk@hongik.ac.kr Tel : +82-2-320-1645 Fax : +82-2-3142-0335

at 2×10^{-2} Torr and 125 W for 2 min. Deep-blue OLEDs were fabricated via the high-vacuum (5×10^{-7} Torr) thermal evaporation of organic materials onto the surface of the ITO-coated glass substrate ($20 \Omega/\text{sq}$; emitting area: 3×3 mm). The deposition rate for all the organic materials was $1.0 \sim 1.1 \text{ \AA}/\text{sec}$, and that for lithium quinolate (Liq) was $0.1 \text{ \AA}/\text{sec}$. Without a vacuum break after the deposition of the organic layers, the Al cathode was deposited at a rate of $10 \text{ \AA}/\text{sec}$. With the DC voltage bias, the optical and electrical properties of the deep-blue OLEDs, such as their current densities, luminances, current efficiencies, and the electroluminescence (EL) spectra of their emission characteristics, were measured, and their EQE and $\text{CIE}_{x,y}$ coordinates were calculated, using Keithley 2400 and CHROMA METER CS-1000A instruments. All the measurements were carried out under ambient conditions, at room temperature.

3. Results and Discussion

Fig. 1 shows the molecular structures of the key materials that were used for fabrication purposes: 2-BCzVBi as the blue dopant, MADN as the blue host (devices A and B), and DNN as the blue host (device B).

Fig. 2(a) shows the two blue device structures that were fabricated in this study: ITO (1500 \AA)/N,N'-bis-(1-naphyl)-N,N'-diphenyl-1,1'-biphenyl-4,4'-diamine (NPB) (400 \AA)/BCzVBi:MADN (5%, 300 \AA) (device A) and BCzVBi:MADN (5%, 150 \AA)/BCzVBi:DNN (5%, 150 \AA) (device B)/ (bis-(2-methyl-8-quinolinolate)-4-(phenylphenolato)aluminum)Alq (BALq) (200 \AA)/Liq (20 \AA)/Al (1000 \AA). Here, NPB, BALq, and Liq were used as the HTL, ETL, and electron injection layer, respectively. The doping concentrations of BCzVBi in MADN (device A) and BCzVBi in MADN and DNN (device B) were optimized to 5%, respectively. The proposed energy level diagrams of device B (with D-EML) are shown in Fig. 2(b). Device A (with S-EML) had a recombination zone (RZ) at the interface of MADN and BALq because MADN and BCzVBi,



Fig. 1. Molecular structure of the key materials that were used for fabrication purposes.

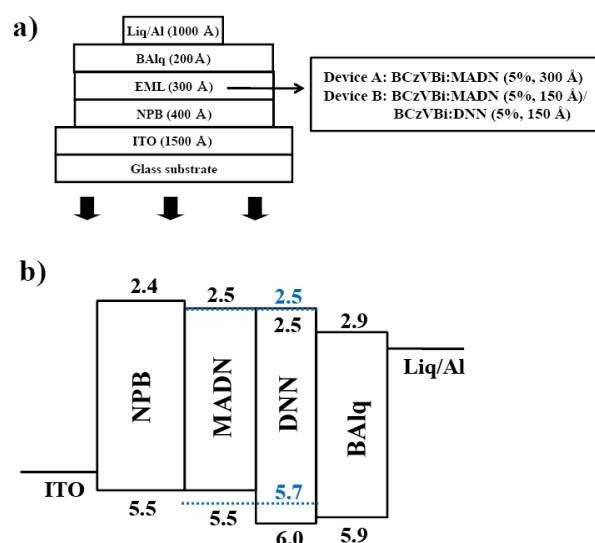


Fig. 2. (a) Structures of the deep-blue OLEDs that were fabricated in this study. (b) Energy level diagrams for device B. The numbers denote the energy level for the HOMO and LUMO of the various materials that were used in this study. The HOMO and LUMO of BCzVBi are represented by the blue dotted line.

which had carbazole derivatives, had ambipolar and hole-transporting properties [14, 15]. Moreover, NPB as HTL had a higher hole mobility ($10^{-4} \text{ cm}^2/\text{V s}$) compared to BALq ($10^{-5} \text{ cm}^2/\text{V s}$) [16, 17]. Device B (with D-EML) had an RZ at the interface of MADN and DNN due to the deep highest occupied molecular orbital (HOMO) of DNN. This indicates that device B (with D-EML) can exploit a broader RZ compared to device A (with S-EML).

Fig. 3 shows the current density vs. voltage and luminance vs. voltage characteristics of devices A and B, respectively. The two devices showed maximum current densities of 289 and 189 mA/cm^2 at 11 V, respectively. Device B had a lower current density at the operating voltage compared to device A. These results indicate that device B had a much larger hole injection barrier (nearly 0.5 or 0.3 eV) between the HOMO of MADN or BCzVBi and the HOMO of DNN compared to S-EML, as shown in Fig. 2(b). Devices A and B had maximum luminances of 3160 and 2900 cd/m^2 at 11 V, respectively.

Fig. 4(a) and (b) show the EQEs and current efficiency vs. luminance characteristics of devices A and B. They had peak EQEs of 2.95 and 4.09% and current efficiencies of 3.67 and 4.47 cd/A at 27.8 and 1.58 cd/m^2 , respectively. The two devices also showed EQEs of 2.02 and 2.74% and current efficiencies of 2.33 and 2.57 cd/A at 1000 cd/m^2 , respectively. Device B (with D-EML) showed a higher effi-

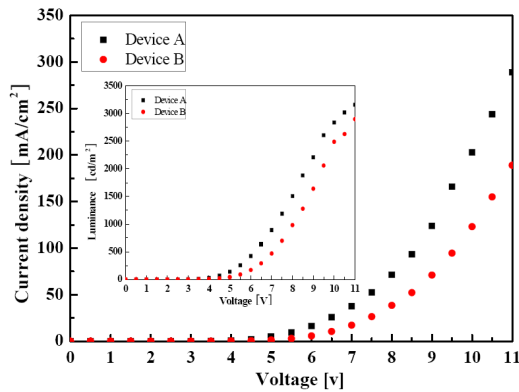


Fig. 3. Current density vs. voltage characteristics of devices A and B. Inset: Luminance vs. voltage characteristics.

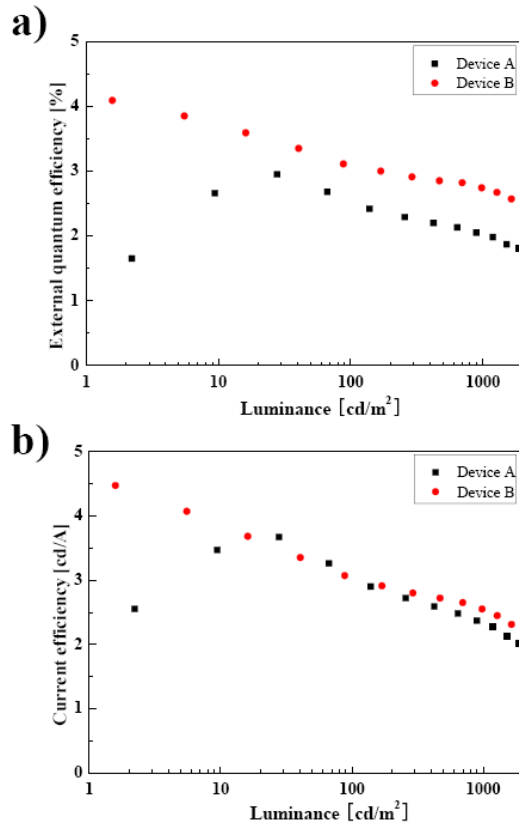


Fig. 4. (a) EQE vs. luminance characteristics of devices A and B. (b) Current efficiency vs. luminance characteristics.

ciency compared to device A (with S-EML) because of the broader RZ of D-EML. A narrow emission zone had a negative effect on the efficiency. Moreover, the Förster energy transfer from DNN to BCzVBi was found to be more efficient than that from MADN because the photoluminescence (PL) spectrum of DNN overlapped better with the ultraviolet (UV)/visible absorption spectrum of BCzVBi compared

to that of MADN, as shown in Fig. 5, which shows the UV/visible absorption spectrum of BCzVBi and the PL spectra of MADN and DNN. Device A exhibited lower efficiency at a low luminance than at a high luminance because of the imbalanced recombination probability of the holes and electrons at a low luminance.

Fig. 6(a) shows the $CIE_{x,y}$ vs. luminance characteristics from 100 to 2000 cd/m^2 of devices A and B. They had an emission of $CIE_{x,y}$ from (0.17, 0.14) and (0.16, 0.11) at 100 cd/m^2 to (0.17, 0.13) and (0.16, 0.10) at 2000 cd/m^2 , respectively. Fig. 6(b) shows the EL spectra of devices A and B from 350 to 650 nm at 1000 cd/m^2 . Devices A and B showed maximum peaks at 444 and 441 nm, respectively, and had full-width half-maximum peaks of 66 and 57 nm, respectively. Both also had deeper-blue emission than BCzVBi did [15, 18]. Incomplete energy transfer from the host to the dopant is necessary for proper color purity. Device B exhibited deeper-blue emission compared to device A because DNN had a larger band gap compared to MADN.

The various characteristics of all the devices are summarized in Table 1, such as their peak EQEs, peak current

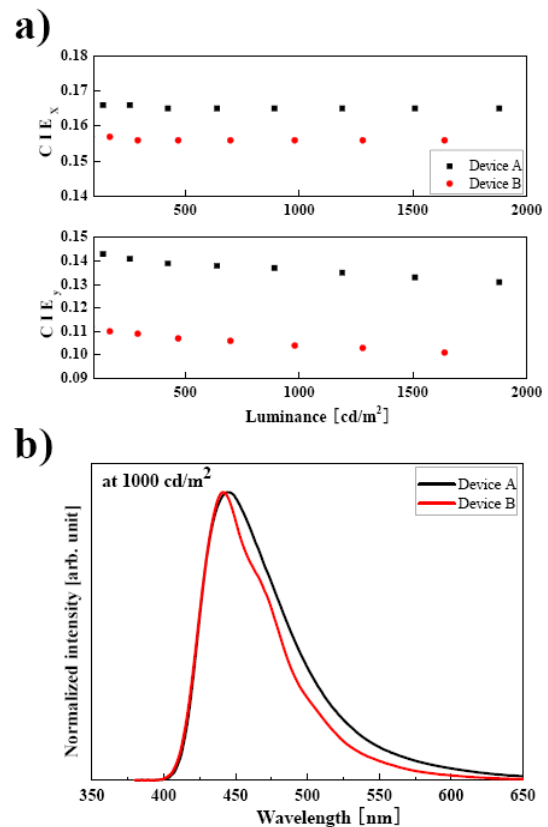


Fig. 6. (a) $CIE_{x,y}$ coordinates of devices A and B from 100 to 2000 cd/m^2 . (b) EL spectra of devices A and B at 1000 cd/m^2 .

Table 1. Various Characteristics of the Deep-Blue OLEDs, including Their Peak EQEs, Peak Current Efficiencies, Peak Power Efficiencies, FWHMs, and CIE_{x,y} Coordinates at 1000 cd/m², Respectively

	Peak EQE [%]	Peak Current Efficiency [cd/A]	Peak Power Efficiency [lm/W]	FWHM [nm]	CIE _{x,y} Coordinates at 1000 cd/m ²
Device A	2.95	3.67	4.01	66	(0.17, 0.14)
Device B	4.47	4.47	3.11	57	(0.16, 0.10)

efficiencies, peak power efficiencies, FWHMs, and CIE_{x,y} coordinates at 1000 cd/m², respectively.

4. Conclusions

In conclusion, deep-blue OLEDs were successfully demonstrated in this study by introducing an emitter of the BCzVBi and D-EML system of MADN and DNN. The D-EML system exhibited good confinement of the holes and electrons within the EML, and a broad recombination zone. The optimized device showed a peak current efficiency of 4.47 cd/A, a peak external quantum efficiency of 4.09%, and *Commission Internationale de L'Eclairage* coordinates of (0.16, 0.10).

References

- [1] J. C. W. Tang and S. A. Van Slyke, *Appl. Phys. Lett.* **51**, 913 (1987).
- [2] J. H. Seo, J. H. Kim, J. H. Seo, G. W. Hyung, J. H. Park, K. H. Lee, S. S. Yoon, and Y. K. Kim, *Appl. Phys. Lett.* **90**, 203507 (2007).
- [3] B. W. D'Andrade and S. R. Forrest, *Adv. Mater.* **16**, 1585 (2004).
- [4] J. J. Kido, M. Kimura, and K. Nagai, *Science*, **267**, 1332 (1995).
- [5] S. Reineke, F. Lindner, G. Schwartz, N. Seidler, K. Walzer, B. Lüssem, and K. Leo, *Nature*, **459**, 234 (2009).
- [6] W. S. Jeon, T. J. Park, S. Y. Kim, R. Pode, J. Jang, and J. H. Kwon, *Appl. Phys. Lett.* **93**, 063303 (2008).
- [7] S. H. Kim, J. Jang, and J. Y. Lee, *Appl. Phys. Lett.* **91**, 083511 (2007).
- [8] Y. Kawamura, K. Goushi, J. Brooks, J. J. Brown, H. Sasabe, and C. Adachi, *Appl. Phys. Lett.* **86**, 071104 (2005).
- [9] C. Adachi, M. A. Baldo, M. E. Thompson, and S. R. Forrest, *J. Appl. Phys.* **90**, 5048 (2001).
- [10] S.H. Lim, G.Y. Ryu, J.H. Seo, J.H. Park, S.W. Youn, Y.K. Kim, D.M. Shin, *Ultramicroscopy*, **108**, 1251 (2008)
- [11] S.H. Khong, S. Sivaramakrishnan, R.Q. Png, L.Y. Wong, P.J. Chia, L.L. Chua, P. K. H. Ho, *Adv. Mater.* **17**, 2493 (2005).
- [12] S. H. Eom, Y. Zheng, E. Wrzesniewski, J. W. Lee, N. Chopra, F. So, and J. Xue, *Appl. Phys. Lett.* **94**, 153303 (2009).
- [13] J. H. Lee, C. L. Huang, C. H. Hsiao, M. K. Leung, C. C. Yang, C. C. Chao, *Appl. Phys. Lett.* **94**, 223301 (2009)
- [14] M. H. Ho, Y. S. Wu, S. W. Wen, M. T. Lee, T. M. Chen, C. H. Chen, K. C. Kwok, S. K. So, K. T. Yeung, Y. K. Cheng, and Z. Q. Gao, *Appl. Phys. Lett.* **89**, 252903 (2006).
- [15] C. Hosokawa, H. Higashi, H. Nakamura, and T. Kusumoto, *Appl. Phys. Lett.* **67** 3853 (1995).
- [16] S. Naka, H. Okada, H. Onnagawa, Y. Yamaguchi, T. Tsutsui, *Syn. Metal.* **111**, 331 (2000)
- [17] G. Schwartz, *Doctor Rerum Naturalium, Novel Concepts for High-Efficiency White Organic Light-Emitting Diodes*, p. 75 (2007).
- [18] S. J. Lee, J. S. Park, K. J. Yoon, Y. I. Kim, S. H. Jin, S. K. Kang, Y. S. Gal, S. W. Kang, J. Y. Lee, J. W. Kang, S. H. Lee, H. D. Park, and J. J. Kim, *Adv. Mater.* **18** 3922 (2008).